The Astrophysical Journal Letters, 786:L18 (6pp), 2014 May 10 doi:10.1088/2041-8205/786/2/L18

DISCOVERY OF A ∼250 K BROWN DWARF AT 2 pc FROM THE SUN*

K. L. Luhman[1,2]
[1] Department of Astronomy and Astrophysics, The Pennsylvania State University, University Park, PA 16802, USA; kluhman@astro.psu.edu
[2] Center for Exoplanets and Habitable Worlds, The Pennsylvania State University, University Park, PA 16802, USA
Received 2014 February 7; accepted 2014 March 7; published 2014 April 21

ABSTRACT

Through a previous analysis of multi-epoch astrometry from the *Wide-field Infrared Survey Explorer (WISE)*, I identified WISE J085510.83−071442.5 as a new high proper motion object. By combining astrometry from *WISE* and the *Spitzer Space Telescope*, I have measured a proper motion of $8.1 \pm 0.1''$ yr^{-1} and a parallax of $0.454 \pm 0.045''$ ($2.20^{+0.24}_{-0.20}$ pc) for WISE J085510.83−071442.5, giving it the third highest proper motion and the fourth largest parallax of any known star or brown dwarf. It is also the coldest known brown dwarf based on its absolute magnitude at 4.5 μm and its color in [3.6]–[4.5]. By comparing $M_{4.5}$ with the values predicted by theoretical evolutionary models, I estimate an effective temperature of 225–260 K and a mass of 3–10 $M_{\rm Jup}$ for the age range of 1–10 Gyr that encompasses most nearby stars.

Key words: brown dwarfs – infrared: stars – proper motions – solar neighborhood – stars: low-mass

1. INTRODUCTION

The closest stars to the Sun have played a central role in studies of stellar astrophysics, as well as appealing to the imagination of the general public (Henry et al. 1997). Over the last century, wide-field imaging surveys have been conducted at progressively fainter magnitudes and longer wavelengths, enabling the detection of the Sun's neighbors down to the hydrogen burning limit (e.g., Barnard 1916; Wolf 1919; Ross 1926; Luyten 1979; Lépine & Shara 2005) and into the substellar regime (e.g., Kirkpatrick et al. 1999; Strauss et al. 1999; Burgasser et al. 2004; Burningham et al. 2010). One of the most recent surveys was performed by the *Wide-field Infrared Survey Explorer* (*WISE*; Wright et al. 2010), which obtained mid-infrared (IR) images of the entire sky. Those data have proven to be highly effective at uncovering the coldest brown dwarfs in the vicinity of the Sun (Cushing et al. 2011; Kirkpatrick et al. 2011).

Most of the brown dwarfs found with *WISE* have been selected based on their colors. However, nearby brown dwarfs also can be identified through their large proper motions, which avoids photometric selection biases (e.g., Deacon et al. 2009; Sheppard & Cushing 2009; Artigau et al. 2010; Kirkpatrick et al. 2010; Scholz 2010). This method has been successfully applied to the *WISE* astrometry by measuring motions relative to near-IR surveys (Gizis et al. 2011; Liu et al. 2011; Scholz et al. 2011; Bihain et al. 2013) and within the multiple epochs from *WISE* (Luhman 2013, 2014; Thompson et al. 2013; Wright et al. 2014; Kirkpatrick et al. 2014). The latter data are especially well-suited for finding nearby objects that are too cold to be detected in near-IR surveys. In this Letter, I characterize an object of this kind from my proper motion survey in Luhman (2014),[3] demonstrating that it is one of the Sun's closest neighbors and the coldest known brown dwarf.

2. OBSERVATIONS

2.1. Mid-IR Images from WISE

Between 2010 January 7 and 2011 February 1, *WISE* performed an all-sky imaging survey in bands centered at 3.4, 4.6, 12, and 22 μm, which are denoted as $W1$, $W2$, $W3$, and $W4$, respectively (Wright et al. 2010). Because of the successive depletion of the two cryogen tanks, images were collected through only $W1/W2/W3$ and $W1/W2$ after 2010 August 6 and 2010 September 29, respectively. Each position in the sky was observed $\gtrsim$12 times over a period of $\gtrsim$1 day at intervals of six months. By the end of the 13 month survey, the images for a given location spanned either 6 or 12 months.

In Luhman (2014), I found that WISE J085510.83−071442.5 (hereafter WISE 0855−0714) moved 2.″5 between two epochs of *WISE* images that are separated by six months, which indicates a proper motion that is unusually high among known stars. The *WISE* data for this object were obtained on 2010 May 4 and 2010 November 11 and consisted of 14 and 13 detections, respectively. It has a color of $W1 - W2 = 2.7$ in the *WISE* All-Sky Source Catalog, which implies a spectral type of T6–T8 (Kirkpatrick et al. 2011). Among the publicly available images that encompass WISE 0855−0714, the data at J and K_s from the Visible and Infrared Survey Telescope for Astronomy (VISTA) Hemisphere Survey (PI. McMahon, ID 179.A-2010) provide the best constraints on its nature. These images are found in the first public data release for that survey in the VISTA Science Archive. The VISTA observations were performed on the night of 2010 March 9, which was only two months prior to the first epoch of *WISE* images for WISE 0855−0714. As a result, its expected position in the VISTA images is well-constrained. An object is not detected at that location in the J and K_s data from VISTA, which are shown in Figure 1 for a $1' \times 1'$ area that encompasses WISE 0855−0714. Using the VISTA catalog of sources in the vicinity of WISE 0855−0714, I estimate that a signal-to-noise ratio (S/N) of 3 corresponds to $J \sim 20.3$ and $K_s \sim 18.6$. The resulting color of $J - W2 > 7$ is much redder than the values of 2.5–4 that are exhibited by T6–T8 dwarfs, and instead is indicative of a Y dwarf (Kirkpatrick et al. 2011).

To investigate the discrepancies in the spectral types implied by $W1 - W2$ and $J - W2$, I examined the *WISE* images of WISE

* Based on data from the *Wide-field Infrared Survey Explorer*, the *Spitzer Space Telescope*, Gemini Observatory, and the VISTA Telescope at ESO's Paranal Observatory.

[3] In a subsequent study, Kirkpatrick et al. (2014) also independently identified this high proper motion object.

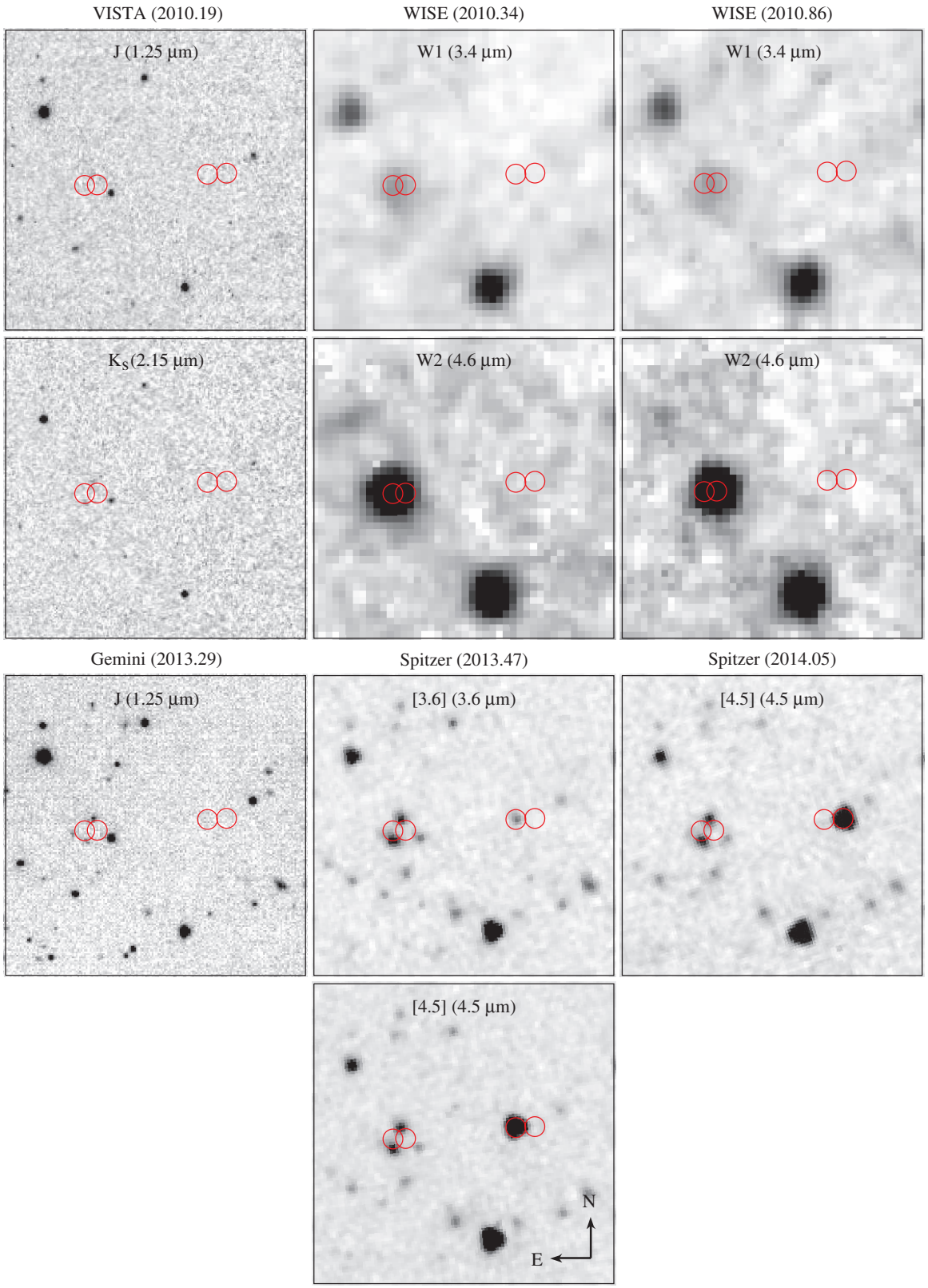

Figure 1. Images of WISE 0855−0714 from VISTA, *WISE*, Gemini, and *Spitzer*. In the *WISE* images, WISE 0855−0714 is a blend of a moving object that dominates at $W2$ and two stationary sources that likely dominate at $W1$. The circles indicate the positions of the moving component in the *WISE* and *Spitzer* images; it is not detected by VISTA or Gemini. The size of each image is $1' \times 1'$.

0855−0714. I retrieved the single exposure images from the NASA/IPAC Infrared Science Archive, and coadded all images at a given filter for each of the two epochs. The resulting images at $W1$ and $W2$ are shown in Figure 1. The mean coordinates of WISE 0855−0714 from the single exposure catalogs in each epoch agree with the positions of the $W2$ source in the coadded images, but each epoch's source in $W1$ is near the midpoint between those coordinates. In other words, the $W2$ source shows

significant movement between epochs while the $W1$ source does not. The position of WISE 0855−0714 in $W1$ is roughly midway between two objects that are near the detection limit in the VISTA K_s image and are separated by 4–5″. Based on these *WISE* and VISTA data, I concluded that WISE 0855−0714 is probably a blend of a moving object that dominates at $W2$ and two stationary sources that dominate at $W1$, which would explain why $W1 - W2$ implies an earlier spectral type than $J - W2$. This scenario is confirmed by the *Spitzer* observations described in Section 2.3. It is unclear which components of WISE 0855−0714 dominate in $W3$, which is available for the first epoch only. The *WISE* All-Sky Source Catalog contains a measurement of photometry for WISE 0855−0714 in $W4$, but no detection is apparent based on visual inspection of the coadded image.

2.2. Near-IR Images from Gemini

I pursued near-IR imaging of WISE 0855−0714 that is deeper than the data from VISTA to better constrain its motion and spectral type and to assess the feasibility of spectroscopy. Among the standard near-IR filters, J and H usually offer the best sensitivity to the coldest brown dwarfs; the former was selected for these observations. The images were obtained with the Gemini Near-Infrared Imager (NIRI) at the Gemini North telescope on the night of 2013 April 17. The instrument contained a 1024×1024 ALADDIN InSb array and was operated with the $f/6$ camera, resulting in a plate scale of 0.″117 pixel^{-1} and a field of view of 2′ × 2′. Twenty-six dithered images of WISE 0855−0714 were collected, each with an exposure time of one minute. The images of WISE 0855−0714 were flat fielded, corrected for distortion, registered, and combined. Astrometry and photometry from VISTA were used to measure the world coordinate system (WCS) and flux calibration for the combined image. Point sources in the image exhibit FWHM ∼ 0.″5. No counterpart to the moving component of WISE 0855−0714 is detected in the NIRI image (see Figure 1). The two components detected by VISTA appear at the same positions in the NIRI image, confirming that they have negligible motion. Using the calibrated photometry for sources in the NIRI image, I estimate that S/N = 3 corresponds to $J \sim 23$.

2.3. Mid-IR Images from Spitzer

Because it was likely to be a new member of the solar neighborhood based on its rapid motion in the *WISE* images, I included WISE 0855−0714 in a survey for common proper motion companions to nearby stars (program 90095) with the *Spitzer Space Telescope* (Werner et al. 2004). For WISE 0855−0714, the data from this program also provide constraints on its colors and motion. It was observed on 2013 June 21 and 2014 January 20 with *Spitzer*'s Infrared Array Camera (IRAC; Fazio et al. 2004). The images in June were collected through the 3.6 and 4.5 μm filters, which are denoted as [3.6] and [4.5]. Because the primary purpose of the second observation was astrometry, only the [4.5] band was employed. Five dithered images were obtained in each filter on a given date. The exposure times for the individual frames were 23.6 and 26.8 s for [3.6] and [4.5], respectively.

The IRAC data were reduced in the manner described by Luhman et al. (2012). The resulting images are shown in Figure 1. IRAC has detected two objects straddling the position of WISE 0855−0714, which coincide with the pair of stationary sources detected by VISTA and NIRI. In the first and second IRAC epochs, the moving component of WISE 0855−0714 appears ∼22″ and 26″ west of its position in the second epoch of *WISE* images, respectively. This object is fainter than the two stationary sources in [3.6], but the opposite is true at [4.5]. Given the similarities in the bandpasses of [3.6]/$W1$ and [4.5]/$W2$, these relative IRAC fluxes confirm the suggestion from Section 2.1 that WISE 0855−0714 is dominated by a moving object in $W2$ and two stationary objects in $W1$. In fact, because $W1$ is fainter than [3.6] for T and Y dwarfs (Kirkpatrick et al. 2011), the dominance of the stationary objects at $W1$ should be even greater than that in [3.6].

Table 1
Parallax, Proper Motion, and Photometry for WISE J085510.83−071442.5

Parameter	Value
π	$0.454 \pm 0.045''$
$\mu_\alpha \cos\delta$	$-8.06 \pm 0.09''$ yr^{-1}
μ_δ	$0.70 \pm 0.07''$ yr^{-1}
J	>23[a]
K_s	>18.6[a,b]
$W1$	>16.4
$W2$	13.89 ± 0.05
$W3$	⩾11.25
$W4$	>9
[3.6]	17.44 ± 0.05
[4.5]	13.89 ± 0.02

Notes. These data apply to the moving component of WISE J085510.83−071442.5. The northern and southern stationary components have [3.6] = 16.70 ± 0.04 and 16.38 ± 0.04 and [4.5] = 16.08 ± 0.04 and 16.05 ± 0.04, respectively.
[a] S/N < 3.
[b] Based on data from the VISTA Hemisphere Survey.

I measured photometry in [3.6] and [4.5] for the moving and stationary components of WISE 0855−0714 from the IRAC images using the methods from Luhman et al. (2012). Those data are presented in Table 1. The $W2$ and [4.5] filters produce photometric magnitudes that agree to within a few percent on average.[4] Therefore, I can estimate the $W2$ photometry of the moving component of WISE 0855−0714 by subtracting the [4.5] photometry of the stationary objects from the $W2$ measurement in the All-Sky Source Catalog ($W2$ = 13.63). The corrected photometry for the moving component is $W2 = 13.89$, which matches the IRAC measurement.

To measure astrometry for the moving component of WISE 0855−0714, I began by measuring pixel coordinates with the task *starfind* in IRAF for all point sources in the reduced [4.5] image from each IRAC epoch and in the coadded $W2$ image from each *WISE* epoch for a 8′ × 8′ field centered on WISE 0855−0714. I used astrometry from the Two Micron All-Sky Survey (2MASS; Skrutskie et al. 2006) for sources in each image to derive offsets in right ascension, declination, and rotation that align the WCS with the 2MASS astrometric system. For each of the *WISE* images, the coordinates measured for WISE 0855−0714 apply to a blend of the moving object and the two stationary sources. To correct for the latter, I added an artificial star with the flux of the moving component to one of the IRAC [4.5] images at a location near the coordinates

[4] http://wise2.ipac.caltech.edu/docs/release/allsky/expsup/sec6_3c.html

Table 2
Astrometry for WISE J085510.83−071442.5

α (J2000) (°)	δ (J2000) (°)	$\sigma_{\alpha,\delta}$ (″)	MJD	Source
133.795224	−7.245138	0.40	55320.4	*WISE*
133.794261	−7.245124	0.40	55511.4	*WISE*
133.788165	−7.244508	0.04	56464.5	*Spitzer*
133.787085	−7.244451	0.04	56677.3	*Spitzer*

Notes. These data apply to the moving component of WISE J085510.83−071442.5. The two stationary components have $\alpha = 133.794680$ and 133.795099, $\delta = -7.244528$ and −7.245711, and $\sigma_{\alpha,\delta} = 0\farcs08$ in the *Spitzer* images.

measured from a given *WISE* epoch, smoothed the resulting image to the resolution of *WISE*, and measured astrometry for the blended source. This process was repeated for artificial stars at different locations until the astrometry of the blend agreed with the *WISE* position. I then adopted the true coordinates of the artificial star for that best fit, which was equivalent to adding $0\farcs2$ and $-0\farcs3$ to the right ascensions measured from the first and second epochs of *WISE* images, respectively. No corrections to the declinations were necessary. To estimate the errors in the astrometry, I computed the standard deviations of the differences in right ascension and declination between the two IRAC epochs and between each *WISE* epoch and 2MASS for sources that have fluxes roughly similar to that of WISE 0855−0714. The implied errors for the *WISE* data are $\sim 0\farcs2$, but I have adopted $0\farcs4$ in an attempt to account for the additional errors introduced by the blending. The astrometric data for the moving component of WISE 0855−0714 from *WISE* and IRAC are listed in Table 2. The coordinates of the stationary components in the IRAC images are included as well. The designation "WISE 0855−0714" refers to the moving object alone in the remainder of this study.

3. CHARACTERIZATION OF WISE 0855−0714

3.1. Parallax and Proper Motion

I applied least-squares fitting of proper and parallactic motion to the astrometry for WISE 0855−0714 with the IDL program MPFIT. The reduced χ^2 for the fit is less than unity (0.3), indicating that the adopted astrometric errors may be overestimated. To check the errors produced by the fitting, I created 1000 sets of astrometry by adding Gaussian noise to the measured values, and fitted parallactic and proper motion to each set. The resulting standard deviations of proper motion and parallax were similar to the errors from MPFIT. The estimates of proper motion and parallax are presented in Table 1. The relative coordinates among the four epochs are shown in Figure 2 after subtraction of the best-fit proper motion.

3.2. Photometric and Physical Properties

To characterize the photometric properties of WISE 0855−0714, I have placed it in diagrams of $J - [4.5]$ versus [3.6]–[4.5] and $M_{4.5}$ versus [3.6]–[4.5] in Figure 3. For comparison, I have included data for known T and Y dwarfs with measured parallaxes and photometry in these bands (Cushing et al. 2011; Dupuy & Liu 2012; Luhman et al. 2012; Tinney et al. 2012; Beichman et al. 2013, 2014; Leggett et al. 2013; Marsh et al. 2013; Kirkpatrick et al. 2013; Dupuy & Kraus 2013). In Figure 3, WISE 0855−0714 is the reddest brown dwarf in

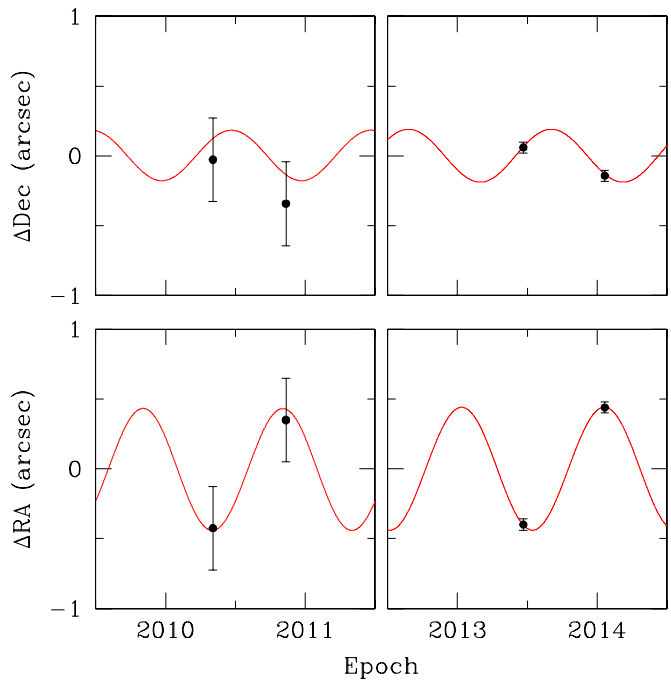

Figure 2. Relative astrometry of WISE 0855−0714 in images from *WISE* (2010) and *Spitzer* (2013–2014) compared to the best-fit model of parallactic motion (Table 1, red curve). The proper motion produced by the fitting has been subtracted.

[3.6]–[4.5] and a contender for the reddest in $J - [4.5]$ with a few Y dwarfs that also lack detections in J. None of the confirmed brown dwarfs that are absent from Figure 3 (e.g., no parallax measurements) have measured [3.6]–[4.5] or $J - [4.5]$ that are redder than the colors of WISE 0855−0714. It is also the faintest known brown dwarf in $M_{4.5}$. These photometric properties indicate that WISE 0855−0714 is the coldest known brown dwarf.

I have estimated the effective temperature of WISE 0855−0714 by comparing its $J - [4.5]$ and $M_{4.5}$ to the predictions of theoretical evolutionary models of brown dwarfs. The color [3.6]–[4.5] was omitted from this exercise because significant errors are likely present in the theoretical fluxes at [3.6] (Leggett et al. 2010). I have used the cloudy models from Burrows et al. (2003) and the versions of the cloudless models from Saumon & Marley (2008) that were utilized by Luhman et al. (2012) in a similar analysis of WD 0806-661 B. I have also employed models by Morley et al. (2014) that include clouds of sulfides, alkali salts, and water ice across 50% of the surface. Since the age of WISE 0855−0714 is unknown, I wish to compare it to model predictions for a span of ages that encompasses most stars in the solar neighborhood, such as 1–10 Gyr. Therefore, I consider the models for 1 and 10 Gyr from Saumon & Marley (2008) and the models for 1 and 5 Gyr from Burrows et al. (2003) (who did not perform calculations beyond 5 Gyr). For $T < 300$ K, the curve of $M_{4.5}$ versus temperature from Morley et al. (2014) changes very little with age, so I use their models for a single surface gravity of $\log g = 4.0$ (∼1–3 Gyr for 200–300 K). The predicted values of $J - [4.5]$ and $M_{4.5}$ are plotted as a function of temperature in Figure 3. The constraints on $J - [4.5]$ and $M_{4.5}$ for WISE 0855−0714 indicate temperatures of $\lesssim$300 K and 225–260 K, respectively, based on the full set of models, and $\lesssim$275 K and 240–260 K according to the new calculations from Morley et al. (2014). Although the [3.6] band was excluded from the temperature analysis because its model

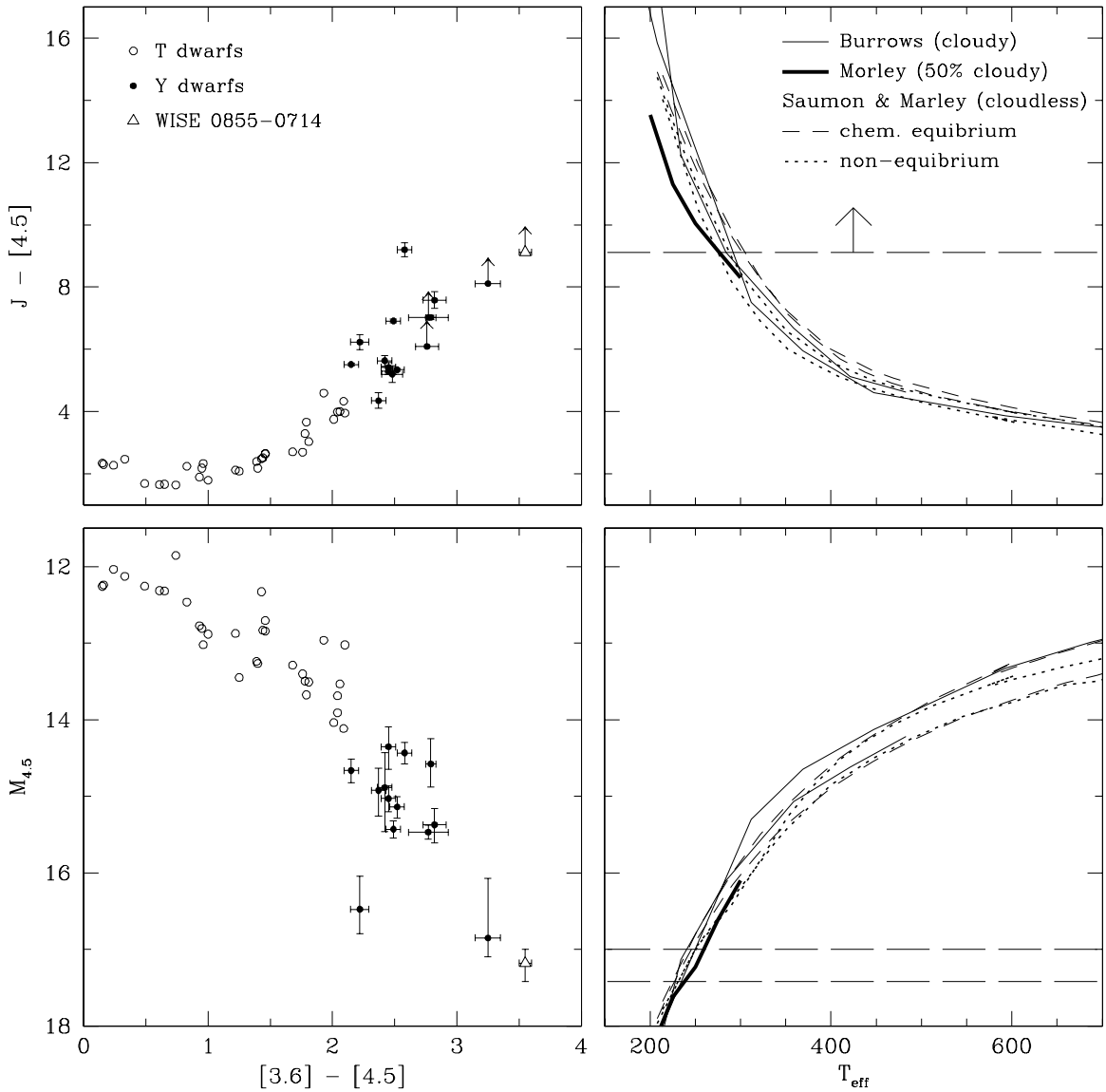

Figure 3. Left: color–magnitude and color–color diagrams for WISE 0855−0714 (open triangle) and samples of T dwarfs (open circles; Dupuy & Liu 2012 and references therein) and Y dwarfs (filled circles; Cushing et al. 2011; Luhman et al. 2012; Tinney et al. 2012; Beichman et al. 2013, 2014; Leggett et al. 2013; Marsh et al. 2013; Kirkpatrick et al. 2013; Dupuy & Kraus 2013). Error bars are included for WISE 0855−0714 and the Y dwarfs. Right: predicted $J - [4.5]$ and $M_{4.5}$ as a function of effective temperature from Burrows et al. (2003; solid lines, 1 and 5 Gyr), Saumon & Marley (2008; short dashed and dotted lines, 1 and 10 Gyr), and Morley et al. (2014; thick solid lines, log $g = 4.0$, ∼1–3 Gyr). The constraints on $J - [4.5]$ and $M_{4.5}$ for WISE 0855−0714 are indicated (long dashed lines).

fluxes may have large errors, I note that if the temperature is derived from the sum of the [3.6] and [4.5] fluxes, the resulting range of values is shifted higher by only ∼2 K from that produced by [4.5] alone. The temperature changes negligibly because [4.5] dominates the sum of the two bands.

The mass of WISE 0855−0714 can be estimated by comparing the observed and theoretical values of $M_{4.5}$. The combination of the models from Burrows et al. (2003) and Saumon & Marley (2008) enable an estimate of the full range of possible masses for 1–10 Gyr. The faint limit for $M_{4.5}$ corresponds to 3 $M_{\rm Jup}$ using the models from Burrows et al. (2003) for 1 Gyr while the bright limit implies 10 $M_{\rm Jup}$ according to the models from Saumon & Marley (2008) for 10 Gyr.

4. DISCUSSION

WISE 0855−0714 has the third highest proper motion of any known object outside the solar system ($\mu = 8\farcs1\,{\rm yr}^{-1}$), behind only Barnard's star (Barnard 1916, $\mu = 10\farcs3\,{\rm yr}^{-1}$) and Kapteyn's star (Kapteyn 1897, $\mu = 8\farcs6\,{\rm yr}^{-1}$). The four closest systems to the Sun known prior to this study are α Cen AB and Proxima Cen (1.338 ± 0.002, 1.296 ± 0.004 pc; Söderhjelm 1999; van Leeuwen 2007), Barnard's star (1.834 ± 0.001 pc; Benedict et al. 1999), WISE J104915.57−531906.1 AB (2.02 ± 0.02 pc; Luhman 2013; Boffin et al. 2014), and Wolf 359 (2.386 ± 0.012 pc; van Altena et al. 1995). With a parallactic distance of $2.20^{+0.24}_{-0.20}$ pc, WISE 0855−0714 likely ranks fourth in proximity to the Sun.

Among known T and Y dwarfs, WISE 0855−0714 is the reddest in [3.6]–[4.5], a contender for the reddest in $J - [4.5]$, and the faintest in $M_{4.5}$, indicating that it is the coldest known brown dwarf (and hence a Y dwarf). When compared to the model predictions of Burrows et al. (2003), Saumon & Marley (2008), and Morley et al. (2014), the constraints on $J - [4.5]$ and $M_{4.5}$ imply effective temperatures of $\lesssim$300 K and 225–260 K, respectively. If it is within the age range of 1–10 Gyr that

encompasses most nearby stars, then it should have a mass of 3–10 $M_{\rm Jup}$ according to the theoretical values of $M_{4.5}$. At this mass, WISE 0855−0714 could be either a brown dwarf or a gas giant planet that was ejected from its system. The former seems more likely given that the frequency of planetary-mass brown dwarfs is non-negligible[5] while the frequency of ejected planets is unknown. Assuming that WISE 0855−0714 is a Y dwarf, the four closest known systems now consist of two M dwarfs and one member of every other spectral type from G through Y.

WISE 0855−0714 offers an opportunity to test atmospheric models in an unexplored temperature regime. Exploiting this opportunity will require additional astrometry to refine its parallax measurement and deeper near-IR photometry to better constrain its spectral energy distribution. Spectroscopy will be necessary for detailed tests of the model atmospheres, but given the current limits on the near-IR fluxes ($J > 23$), it may not be feasible until the deployment of the *James Webb Space Telescope*.

I acknowledge support from grant NNX12AI47G from the NASA Astrophysics Data Analysis Program. I thank Caroline Morley and Didier Saumon for providing their model calculations. *WISE* is a joint project of UCLA and JPL/Caltech, funded by NASA. The Gemini data were obtained through program GN-2013A-DD-3. Gemini Observatory is operated by AURA under a cooperative agreement with the NSF on behalf of the Gemini partnership: the NSF (United States), the NRC (Canada), CONICYT (Chile), the ARC (Australia), Ministério da Ciência, Tecnologia e Inovação (Brazil) and Ministerio de Ciencia, Tecnología e Innovación Productiva (Argentina). 2MASS is a joint project of the University of Massachusetts and IPAC at Caltech, funded by NASA and the NSF. The Center for Exoplanets and Habitable Worlds is supported by the Pennsylvania State University, the Eberly College of Science, and the Pennsylvania Space Grant Consortium.

REFERENCES

Alves de Oliveira, C., Moraux, E., Bouvier, J., & Bouy, H. 2012, A&A, 539, A515
Artigau, É., Radigan, J., Folkes, S., et al. 2010, ApJL, 718, L38
Barnard, E. E. 1916, AJ, 29, 181
Beichman, C., Gelino, C. R., Kirkpatrick, J. D., et al. 2013, ApJ, 764, 101
Beichman, C., Gelino, C. R., Kirkpatrick, J. D., et al. 2014, ApJ, 783, 68
Benedict, G. F., McArthur, B., Chappell, D. W., et al. 1999, AJ, 118, 1086
Bihain, G., Scholz, R.-D., Storm, J., & Schnurr, O. 2013, A&A, 557, A43
Boffin, H. M. J., Pourbaix, D., Mužić, K., et al. 2014, A&A, 561, L4
Burgasser, A. J., McElwain, M. W., Kirkpatrick, J. D., et al. 2004, AJ, 127, 2856
Burningham, B., Pinfield, D. J., Lucas, P. W., et al. 2010, MNRAS, 406, 1885
Burrows, A., Sudarsky, D., & Lunine, J. I. 2003, ApJ, 596, 587
Cushing, M. C., Kirkpatrick, J. D., Gelino, C. R., et al. 2011, ApJ, 743, 50
Deacon, N. R., Hambly, N. C., King, R. R., & McCaughrean, M. J. 2009, MNRAS, 394, 857
Dupuy, T. J., & Kraus, A. L. 2013, Sci, 341, 1492
Dupuy, T. J., & Liu, M. C. 2012, ApJS, 201, 19
Fazio, G. G., Hora, J. L., Allen, L. E., et al. 2004, ApJS, 154, 10
Gizis, J. E., Troup, N. W., & Burgasser, A. J. 2011, ApJL, 736, L34
Henry, T. J., Ianna, P. A., Kirkpatrick, J. D., & Jahreiss, H. 1997, AJ, 114, 388
Kapteyn, J. C. 1897, AN, 145, 159
Kirkpatrick, J. D., Cushing, M. C., Gelino, C. R., et al. 2011, ApJS, 197, 19
Kirkpatrick, J. D., Cushing, M. C., Gelino, C. R., et al. 2013, ApJ, 776, 128
Kirkpatrick, J. D., Looper, D. L., Burgasser, A. J., et al. 2010, ApJS, 190, 100
Kirkpatrick, J. D., Reid, I. N., Liebert, J., et al. 1999, ApJ, 519, 802
Kirkpatrick, J. D., Schneider, A., Fajardo-Acosta, S., et al. 2014, ApJ, 783, 122
Leggett, S. K., Burningham, B., Saumon, D., et al. 2010, ApJ, 710, 1627
Leggett, S. K., Morley, C. V., Marley, M. S., et al. 2013, ApJ, 763, 130
Lépine, S., & Shara, M. M. 2005, AJ, 129, 1483
Liu, M. C., Deacon, N. R., Magnier, E. A., et al. 2011, ApJL, 740, L32
Luhman, K. L. 2013, ApJL, 767, L1
Luhman, K. L. 2014, ApJ, 781, 4
Luhman, K. L., Burgasser, A. J., Labbé, I., et al. 2012, ApJ, 744, 135
Luyten, W. J. 1979, LHS Catalogue, A Catalogue of Stars with Proper Motions Exceeding 0"5 Annually (2nd ed.; Minneapolis, MN: Univ. Minnesota)
Marsh, K. A., Wright, E. L., Kirkpatrick, J. D., et al. 2013, ApJ, 762, 119
Morley, C. V., Marley, M. S., Fortney, J. J., et al. 2014, ApJ, in press
Ross, F. E. 1926, AJ, 36, 124
Saumon, D., & Marley, M. S. 2008, ApJ, 689, 1327
Scholz, R.-D. 2010, A&A, 515, A92
Scholz, R.-D., Bihain, G., Schnurr, O., & Storm, J. 2011, A&A, 532, L5
Sheppard, S. S., & Cushing, M. C. 2009, AJ, 137, 304
Skrutskie, M., Cutri, R. M., Stiening, R., et al. 2006, AJ, 131, 1163
Söderhjelm, S. 1999, A&A, 341, 121
Strauss, M. A., Fan, X., Gunn, J. E., et al. 1999, ApJL, 522, L61
Thompson, M. A., Kirkpatrick, J. D., Mace, G. N., et al. 2013, PASP, 125, 809
Tinney, C. G., Faherty, J. K., Kirkpatrick, J. D., et al. 2012, ApJ, 759, 60
van Altena, W. F., Lee, J. T., & Hoffleit, E. D. 1995, The General Catalogue of Trigonometric Stellar Parallaxes (4th ed.; New Haven, CT: Yale Univ. Obs.)
van Leeuwen, F. 2007, A&A, 474, 653
Werner, M. W., Roellig, T. L., Low, F. J., et al. 2004, ApJS, 154, 1
Wolf, M. 1919, VeHei, 7, 195
Wright, E. L., Eisenhardt, P. R. M., Mainzer, A. K., et al. 2010, AJ, 140, 1868
Wright, E. L., Kirkpatrick, J. D., Gelino, C. R., et al. 2014, AJ, 147, 61

[5] This is based on surveys of star-forming regions (e.g., Alves de Oliveira et al. 2012), which are young enough that planet ejection is unlikely to have occurred at a significant level.